Foldamer Heterodimerization

DOI: 10.1002/ange.201407752

Increasing the Size of an Aromatic Helical Foldamer Cavity by Strand Intercalation**

*Michael L. Singleton, Geert Pirotte, Brice Kauffmann, Yann Ferrand, and Ivan Huc**

Abstract: *The postsynthetic modulation of capsules based on helical aromatic oligoamide foldamers would be a powerful approach for controlling their receptor properties without altering the initial monomer sequences. With the goal of developing a method to increase the size of a cavity within a helix, a single-helical foldamer capsule was synthesized with a wide-diameter central segment that was designed to intercalate with a second shorter helical strand. Despite the formation of stable double-helical homodimers ($K_{dim} > 10^7\,M^{-1}$) by the shorter strand, when it was mixed with the single-helical capsule sequence, a cross-hybridized double helix was formed with $K_a > 10^5\,M^{-1}$. This strategy makes it possible to direct the formation of double-helical heterodimers. On the basis of solution- and solid-state structural data, this intercalation resulted in an increase in the central-cavity size to give a new interior volume of approximately 150 Å^3.*

Aromatic helical foldamers are a rapidly growing class of oligomers that can provide cavities for the recognition of guest molecules or ions through self-organization.[1] These molecular strands, which consist of well-defined sequences of monomeric building blocks, give rise to novel, bioinspired, highly tunable synthetic receptors through a specifically programmed folding process. By establishing rational codes between the primary sequences and helically folded secondary structures, the molecular-recognition properties of foldamer receptors can be designed through proper monomer choice. Indeed, each monomer makes a predictable contribution to strand curvature, which determines cavity size, and to the interior array of functional groups, which contributes to guest binding. Over the last decade, a variety of foldamer receptors have been described on the basis of various designs, including open-ended helices or shaped-persistent macrocycles that may bind to small[2] or dumbbell-shaped[3] guests, closed helical capsules terminated by narrow helical segments,[4,5] double-helical capsules,[4,6] and sequences with two enantiomeric binding sites.[7]

Folding is a dynamic process that may be influenced by external stimuli. In the case of aromatic foldamer backbones, possible external stimuli include light,[8] a change in the pH value,[9] and metal binding.[10] The resulting triggered conformational changes may endow aromatic foldamer receptors with controlled-release or guest-swapping properties.[11] In this context, we introduce herein a conceptually novel strategy for postsynthetic modulation of the size and properties of a foldamer cavity. The central part of a single-helical foldamer capsule with a wide diameter at its center and narrower helical segments at each end may be able to intercalate with a distinct shorter helical strand to form a local double helix (Figure 1a). The outcome of this process would be a springlike extension of the capsule and a resulting large increase in—possibly a doubling of—the volume of the cavity, as well as the addition to the cavity wall of any functionality carried by the inner rim of the intercalating strand. Such selective heteromeric dimerization would thus open up new possibilities for foldamer-based guest binding and release, and would contrast strongly with other examples of synthetic heteromeric organic duplexes.[12]

This concept stemmed from our recurrent observation that enlargement of the helix diameter of helical aromatic oligoamide foldamers strongly enhances their ability to intertwine into multistranded complexes, including duplexes, triplexes, and quadruplexes.[13] Although this property is taken advantage of in this case, it was initially considered as an impediment to the formation of well-defined single-helical capsules.[14] Consequently, quinoline-based trimeric[5] or longer[15] segments—a design with a narrow helix diameter that prevents multiple-helix formation—were introduced at the end of capsule sequences not only to serve as end caps, but also to prevent their self-association. However, we reasoned that the inability of the quinoline segments to form multistranded helices may not keep the central part of a capsule from self-hybridizing with a shorter strand. Because it would lack the same quinoline segments, this shorter strand would be expected to self-hybridize. Nevertheless, the equilibrium between two single-helical capsules plus a duplex of the short strand, and two capsules each with a short strand intercalated

[*] Dr. M. L. Singleton, G. Pirotte, Dr. Y. Ferrand, Dr. I. Huc
Université de Bordeaux, CBMN, UMR5248
Institut Européen de Chimie et Biologie
2 rue Escarpit, 33600 Pessac (France)
and
CNRS, CBMN, UMR5248 (France)
E-mail: i.huc@iecb.u-bordeaux.fr
Dr. B. Kauffmann
Université de Bordeaux, UMS3033
Institut Européen de Chimie et Biologie (IECB)
2 rue Escarpit, 33600 Pessac (France)
and
CNRS, IECB, UMS3033 (France)
and
INSERM, IECB, UMS3033 (France)

[**] This research was supported by the Seventh Framework Programme of the European Union through Marie Curie Actions (PIIF-GA-2010-275209, postdoctoral fellowship to M.L.S.) and by the Fondation Simone et Cino Del Duca de l'Institut de France (postdoctoral fellowship to M.L.S.). We thank Prof. A. J. Wilson for fruitful preliminary discussions on the concept described herein and C. Tsiamantas for providing the Q_4 amine units.

Supporting information for this article is available on the WWW under http://dx.doi.org/10.1002/anie.201404452.

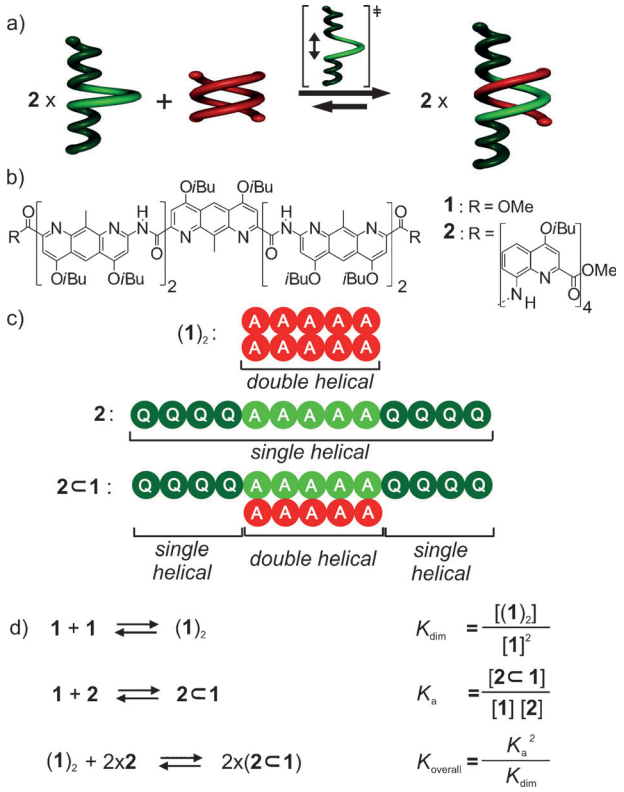

Figure 1. a) Intercalation of a helical segment with a wide diameter and a propensity to self-hybridize into duplexes (in red) into a longer sequence that exists as a single helix (in green) to form a heteroduplex. b) Structures of oligomers **1** and **2**. c) Simplified color-coded representation of the double helix $(\mathbf{1})_2$, the single helix **2**, and their corresponding cross-hybridized double helix **2**⊂**1**. **Q** stands for 8-amino-2-quinolinecarboxylic acid monomers and **A** for both 1,8-diaza-9-methyl-2,7-anthracenedicarboxylic acid and 7-amino-1,8-diaza-9-methyl-2-anthracenecarboxylic acid monomers. d) Equilibria involved in the association of **1** and **2**, and corresponding equilibrium constants.

(Figure 1a), might be expected to favor the latter. Indeed, this equilibrium is governed by the ratio between the dimerization constant of the short strand and the square of its association constant to the single-helical capsule (Figure 1d). In other words, even though short-strand dimerization may be intrinsically stronger than its intercalation, the latter may be favored because it occurs twice at the expense of a unique duplex-dissociation event. In essence, heterodimerization would be favored by a principle of maximal site occupancy similar to that well-known in coordination chemistry.[16]

We designed aromatic oligoamides **1** and **2** (Figure 1b,c) to test these hypotheses. Both contain a pentameric $\mathbf{A}_5$ segment expected to fold into a helix with a wide diameter according to well-established principles,[1a] and also to promote hybridization.[13] However, the peripheral $\mathbf{Q}_4$ segments in **2** should prevent self-hybridization, in addition to capping the central cavity.[5,15] These sequences are the first to include 1,8-diazaanthracene-based amino acids, which were recently developed to contain various functionalities in the 9-position, that is, at the inner rim of aromatic foldamer helices.[17] In the context of this case study, simple methyl groups were used.

For the synthesis of pentamer **1**, the starting monomer was first deprotected (Boc groups removed) or saponified, and the resulting amine and acid were coupled by using (benzotriazol-1-yloxy)tripyrrolidinophosphonium hexafluorophosphate (PyBOP) to give a dimer (see the Supporting Information). The amine on the dimer was then deprotected and coupled to a central diacid.

The anticipated strong propensity of **1** to self-hybridize into stable multihelical structures was validated by a variety of solution-based evidence. At a concentration of 1 mM in $CDCl_3$, a solvent known to favor the hybridization of aromatic oligoamides, the ^{1}H NMR spectrum showed one set of signals (Figure 2a). In agreement with the expected symmetry of the

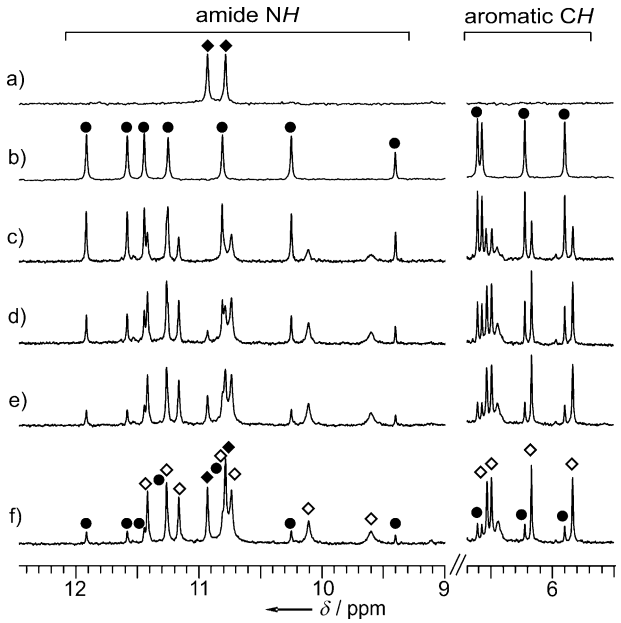

Figure 2. ^{1}H NMR spectra in $CDCl_3$ of a) **1** (1 mM); b) **2** (1 mM); c) **2** with **1** (0.5 equiv); d) **2** with **1** (1.0 equiv); e) **2** with **1** (1.5 equiv); f) **2** with **1** (2.0 equiv). Resonances for each species are indicated in (f) by ◆ ($(\mathbf{1})_2$), ● (**2**), and ◇ (**2**⊂**1**).

molecule, the signal of the hydrogen atom at the 10-position of the central monomer was identified on the basis of its integration at half the value found for the other aromatic and amide resonances. This signal ($\delta = 7.79$ ppm) is shifted significantly upfield relative to the resonances of similar hydrogen atoms in shorter diazaanthracene precursors ($\delta =$ 9.08–8.90 ppm), which is consistent with a ring-current effect resulting from π–π stacking interactions of a nearby aromatic ring.[13] However, intramolecular stacking near the central monomer can be excluded in the single-helical conformation of **1** because its expected length spans less than 1.5 turns and therefore points to a multihelical structure. Upon heating in $C_2D_2Cl_4$, this signal shifted downfield as the multistranded structure dissociated (see Figure S1 in the Supporting Information). Further support came from the NOESY spectrum of **1**, which showed a correlation between the signal of the hydrogen atom at the 10-position of the central diazaanthracene unit and the overlapping signals of hydrogen atoms at

the 10-position of other diazaanthracene moieties (see Figure S2). In the single helix, these hydrogen atoms should be at least 10 Å apart, whereas in an aggregated state, these hydrogen atoms can be within the range in which NOE transfer occurs. Although these observations could also be consistent with a less-ordered aggregated state, such as stacked columns, the sharp NMR signals hint at a discrete structure.

The ^{1}H NMR spectrum of **1** showed minimal concentration dependence from 5 to 0.5 mM, thus suggesting high stability of the aggregate and the absence of dissociation into a single helix within this concentration range. However, at higher concentrations, a second set of signals emerged at higher fields relative to those of the major species (see Figure S3). On the basis of mass spectral data (see Figure S4), which revealed the presence of both dimeric and trimeric aggregates, and an X-ray crystal structure of double-helical $(\mathbf{1})_2$ (see below), the new signals were tentatively assigned to a triplex $(\mathbf{1})_3$, whereas the major species was assigned as the duplex. The absence of signals for monomeric **1** at a concentration of 0.5 mM in $CDCl_3$ suggests that its proportion is below 1%, thus leading to an estimation of the dimerization constant as higher than $10^7\,M^{-1}$. Upon the addition of [D_5]pyridine to a solution of **1** in $CDCl_3$, a new set of signals emerged at a higher field relative to the signals of the dimer (see Figure S5). By analogy with the spectra recorded at high concentration in $CDCl_3$ and consistent with mass spectra, these new signals were assigned to the triplex $(\mathbf{1})_3$. In agreement with this assignment, the proportion of the double helix was shown to increase upon dilution or upon heating from 30 to 70 °C.

The synthesis of **2** proceeded from a quinoline tetramer $\mathbf{Q}_4$ with a free terminal amine, to which a carboxylic acid terminated dimer $\mathbf{A}_2$ was coupled through in situ acid chloride activation with PPh_3 and trichloroacetonitrile. Amine deprotection of $\mathbf{Q}_4\mathbf{A}_2$ followed by PyBOP coupling with a diazaanthracene diacid gave the tridecameric oligomer **2**. Mass spectral data indicated the monomeric form to be the only significant species, as confirmed by a crystal structure (see below). Furthermore, the ^{1}H NMR signal of the hydrogen atom at the 10-position of the central **A** unit was found at 9.36 ppm, thus indicating a lack of the π–π interactions observed for $(\mathbf{1})_2$. This value is largely concentration-independent and quite similar to that of the precursor sequences, which, because of their short length, cannot exist as multiple helices. However, perhaps the most important evidence for the single-helical nature of **2** is in its interaction with **1**.

Upon the mixing of $(\mathbf{1})_2$ with **2**, the cross-hybridized complex **2**⊂**1** formed preferentially, thus validating our design principles. The addition of **1** to a 1 mM solution of **2** in $CDCl_3$ indeed resulted in a decrease in the intensity of the signals of **2** and in the emergence of a new set of signals, assigned to **2**⊂**1**, whose proportion increased over the course of 30 min as equilibrium was reached (Figure 2c–f; see also Figure S5). The cross-hybrid complex was the major species in an equimolar mixture of **1** and **2** (**2**⊂**1**, **2**, and $(\mathbf{1})_2$ in a 3.8:2:1 ratio), and its proportion with respect to **2** kept increasing upon further addition of **1**. The proportions between the species enabled the calculation of an overall association constant between two molecules of **2** and $(\mathbf{1})_2$ with $K_{overall} \approx 2\times10^4\,M^{-1}$ (see Figure S7). From this value and that estimated above for the dimerization of **1** ($K_{dim} > 10^7\,M^{-1}$), it can be deduced that the association constant, K_a, between **2** and monomeric **1** is higher than $4\times10^5\,M^{-1}$, and that $(K_{dim}/K_a) = (K_a/K_{overall}) > 20$. The association of **1** with **2** is thus intrinsically less favorable than association with itself, but nevertheless remains preferred by the principle of maximal site occupancy.[16]

Evidence that the new complex results from the intercalation of a molecule of **1** into the structure of **2** was found in solution by ESI mass spectrometry and diffusion-ordered spectroscopy (^{1}H DOSY). The DOSY spectrum of an equimolar mixture, [**1**] = [**2**] = 3 mM, indicated a greater solvodynamic radius of **2**⊂**1** relative to that of single-helical **2** (see Figure S8). Two distinct diffusion coefficients, $6.62\times10^{-10}\,m^2s^{-1}$ and $5.73\times10^{-10}\,m^2s^{-1}$, were found, with the larger corresponding to **2** and the smaller corresponding to **2**⊂**1**. Because **1** cannot hybridize with the quinoline groups of **2**, the overall change in size is likely to be a result of intercalation in, and thus of expansion of, the central $\mathbf{A}_5$ segment of **2**. This result and the structures of dimeric $(\mathbf{1})_2$ and monomeric **2** were fully validated in the solid state (Figure 3).

Crystals of **1** and **2** suitable for X-ray crystallographic analysis were obtained by the slow diffusion of hexane into a solution of each compound in $CHCl_3$, whereas for **2**⊂**1**, slow evaporation of $CHCl_3$ from a solution of **2**⊂**1** in DMSO/$CHCl_3$ (1:1) produced the best results. The crystal structure of $(\mathbf{1})_2$ showed that the two strands are oriented at approximately 180° with respect to one another around the helical axis of the duplex, thus leading to almost perfect D_2 symmetry. The double-helix pitch is close to 7.0 Å, which enables the reciprocal intercalation of the two strands, as opposed to a pitch of 3.5 Å in the structure of single-helical **2**. The large size of the **A** units results in a wide diameter of $(\mathbf{1})_2$ (ca. 10 Å across for the inner aromatic rim and 16 Å for the exterior aromatic rim; see Figure S10). It follows that the springlike extension of single-helical **1** to form the duplex is accommodated by an average increase in the tilt angle between adjacent diazaanthracene planes of less than 2° (see Figure S16).[13a]

For **2**, the reason for the disfavored self-association is readily apparent from the crystal structure. The bulk imparted by the peripheral $\mathbf{Q}_4$ segments takes up over half of the cross-section of the $\mathbf{A}_5$ turn and sterically prohibits the addition of a second strand. Interestingly, there is an expansion in the circumference of the $\mathbf{A}_5$ segment in the structure of **2** relative to that of $(\mathbf{1})_2$. In $(\mathbf{1})_2$, each pentameric strand makes up 1.25 turns; the first and last units almost completely overlap when viewed along the helix axis. In contrast, in **2**, the five diazaanthracene units make up slightly more than one turn, with only a single aromatic ring of the first and last diazaanthracene units overlapping (see Figure S16). As a result, the internal diameter of the helix (measured from the 9-methyl carbon atom of the central diazaanthracene monomer to a 9-methyl carbon atom opposite it) increases from 7.3 Å in $(\mathbf{1})_2$ to 9.9 Å in **2**.

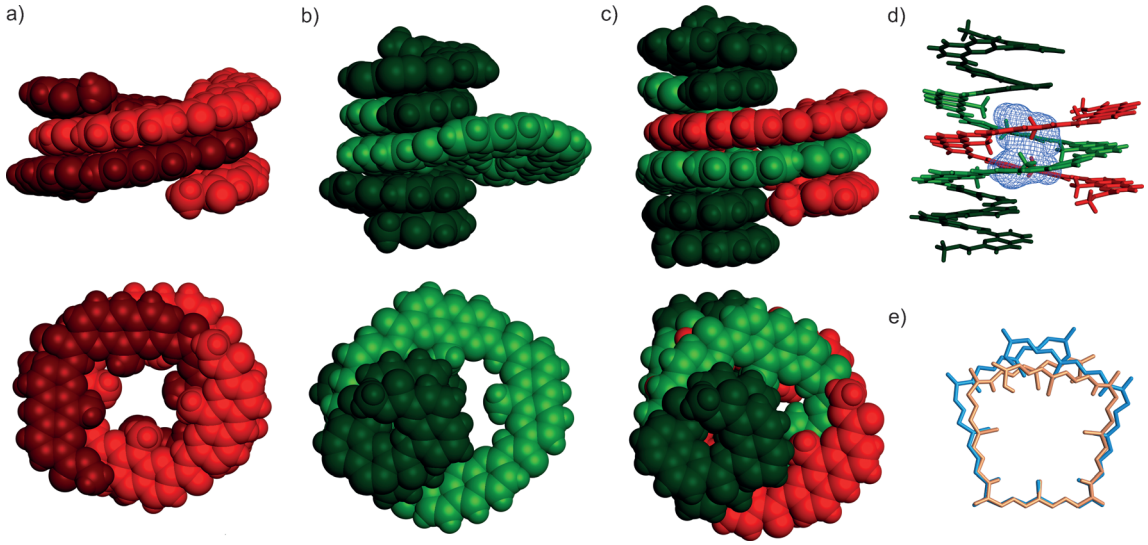

Figure 3. Side (top) and top (bottom) views of the solid-state structure of a) double-helical $(\mathbf{1})_2$, b) single-helical **2**, and c) cross-hybridized double-helical **2**⊂**1** (CPK representations). d) Side view of **2**⊂**1** as a tube representation. The volume created by strand intercalation is shown as a blue isosurface (quad mesh). The strands are color-coded as in Figure 1. For clarity, isobutyl groups and included solvent molecules are not shown. e) Overlay of the inner rim of the $\mathbf{A}_5$ segment of **2** (blue) and one $\mathbf{A}_5$ segment of $(\mathbf{1})_2$ (orange).

The structure of **2**⊂**1** shows the expected intercalation of a single strand of **1** in the central $\mathbf{A}_5$ segment of **2** to yield a double-helical portion that is similar to the structure of $(\mathbf{1})_2$. The length of the cavity of **2**⊂**1** relative to the helical axis is increased as a result of the change in helical pitch from 3.5 to approximately 7 Å (Figure 3d). A slight constriction in the circumference of the cavity of **2**⊂**1** is also observed (Figure 3e). The decrease in diameter relative to **2** is approximately 2.5 Å, similar to that observed in $(\mathbf{1})_2$. Nevertheless, the cavity in **2**⊂**1** remains relatively large, with an interior volume of 150 Å^3. One additional feature that the intercalation brings to the cavity is the array of methyl groups provided by each unit of **1**. Although these groups offer little more than bulk in the context of this test-case study, the incorporation of diazaanthracene units with diverse functional groups[17,18] would be useful for applications in molecular recognition. Thus, this strategy for cavity modification could be used to alter both the size of the receptor site and its internal electrostatic potential surface.

In conclusion, we have described the initial synthesis and characterization of oligomers consisting of long sequences of diazaanthracene amino acid monomers. The ability of these oligomers to form multiple helices was studied and controlled by use of the previously established strategy of incorporating bulky helical end caps to prevent self-association. By using these units, it was found that an aromatic oligoamide foldamer capsule possessing a large-diameter central sequence with narrow helical units on each end still retains its ability to form multiple helices with a foldamer sequence lacking the narrow end groups. This approach offers a novel way to postsynthetically modify the size of a foldamer-based cavity and could eventually be used to control guest association and release. The reliance of this method on the inherent ability of the large aromatic units to hybridize makes it potentially applicable to a range of aromatic sequences consisting of different monomers that have been shown to hybridize into multihelical structures.[13] Studies focused on the application of this strategy to the modification of helical aromatic oligoamide receptors are currently under way.

Received: July 20, 2014
Published online: October 3, 2014

Keywords: capsules · crystallography · foldamers · helical structures · supramolecular chemistry

[1] For reviews, see: a) D.-W. Zhang, X. Zhao, J.-L. Hou, Z.-T. Li, *Chem. Rev.* **2012**, *112*, 5271 – 5316; b) G. Guichard, I. Huc, *Chem. Commun.* **2011**, *47*, 5933 – 5941; c) H. Juwarker, K.-S. Jeong, *Chem. Soc. Rev.* **2010**, *39*, 3664 – 3674; d) I. Saraogi, A. D. Hamilton, *Chem. Soc. Rev.* **2009**, *38*, 1726 – 1743.

[2] a) K.-J. Chang, B.-N. Kang, M.-H. Lee, K.-S. Jeong, *J. Am. Chem. Soc.* **2005**, *127*, 12214 – 12215; b) M. Waki, H. Abe, M. Inouye, *Angew. Chem. Int. Ed.* **2007**, *46*, 3059 – 3061; *Angew. Chem.* **2007**, *119*, 3119 – 3121; c) Y.-X. Xu, X. Zhao, X.-K. Jiang, Z.-T. Li, *J. Org. Chem.* **2009**, *74*, 7267 – 7273; d) J.-L. Hou, X.-B. Shao, G.-J. Chen, Y.-X. Zhou, X.-K. Jiang, Z.-T. Li, *J. Am. Chem. Soc.* **2004**, *126*, 12386 – 12394; e) H. L. Fu, Y. Liu, H. Q. Zeng, *Chem. Commun.* **2013**, *49*, 4127 – 4144; f) H. Q. Zhao, J. Shen, J. J. Guo, R. J. Ye, H. Q. Zeng, *Chem. Commun.* **2013**, *49*, 2323 – 2325; g) Y. Ferrand, Q. Gan, B. Kauffmann, H. Jiang, I. Huc, *Angew. Chem. Int. Ed.* **2011**, *50*, 7572 – 7575; *Angew. Chem.* **2011**, *123*, 7714 – 7717.

[3] a) T. Nishinaga, A. Tanatani, K. Oh, J. S. Moore, *J. Am. Chem. Soc.* **2002**, *124*, 5934 – 5935; b) A. Tanatani, T. S. Hughes, J. S. Moore, *Angew. Chem. Int. Ed.* **2002**, *41*, 325 – 328; *Angew. Chem.* **2002**, *114*, 335 – 338; c) A. Petitjean, L. A. Cuccia, M. Schmutz, J.-M. Lehn, *J. Org. Chem.* **2008**, *73*, 2481 – 2495; d) Q. Gan, Y. Ferrand, C. Bao, B. Kauffmann, A. Grélard, H. Jiang, I. Huc, *Science* **2011**, *331*, 1172 – 1175; e) Q. Gan, Y. Ferrand, N. Chandramouli, B. Kauffmann, C. Aube, D. Dubreuil, I. Huc, *J. Am. Chem. Soc.* **2012**, *134*, 15656 – 15659.

[4] Y. Hua, Y. Liu, C.-H. Chen, A. H. Flood, *J. Am. Chem. Soc.* **2013**, *135*, 14401 – 14412.
[5] a) J. Garric, J.-M. Léger, I. Huc, *Angew. Chem. Int. Ed.* **2005**, *44*, 1954 – 1958; *Angew. Chem.* **2005**, *117*, 1990 – 1994; b) C. Bao, B. Kauffmann, Q. Gan, K. Srinivas, H. Jiang, I. Huc, *Angew. Chem. Int. Ed.* **2008**, *47*, 4153 – 4156; *Angew. Chem.* **2008**, *120*, 4221 – 4224; c) Y. Ferrand, A. M. Kendhale, B. Kauffmann, A. Grélard, C. Marie, V. Blot, M. Pipelier, D. Dubreuil, I. Huc, *J. Am. Chem. Soc.* **2010**, *132*, 7858 – 7859.
[6] C. Bao, Q. Gan, B. Kauffmann, H. Jiang, I. Huc, *Chem. Eur. J.* **2009**, *15*, 11530 – 11536.
[7] G. Lautrette, B. Kauffmann, Y. Ferrand, C. Aube, N. Chandramouli, D. Dubreuil, I. Huc, *Angew. Chem. Int. Ed.* **2013**, *52*, 11517 – 11520; *Angew. Chem.* **2013**, *125*, 11731 – 11734.
[8] a) C. Tie, J. C. Gallucci, J. R. Parquette, *J. Am. Chem. Soc.* **2006**, *128*, 1162 – 1171; b) Z. Yu, S. Hecht, *Angew. Chem. Int. Ed.* **2011**, *50*, 1640 – 1643; *Angew. Chem.* **2011**, *123*, 1678 – 1681; c) Z. Yu, S. Hecht, *Chem. Eur. J.* **2012**, *18*, 10519 – 10524.
[9] a) E. Kolomiets, V. Berl, I. Odriozola, A.-M. Stadler, N. Kyritsakas, J.-M. Lehn, *Chem. Commun.* **2003**, 2868 – 2869; b) C. Dolain, V. Maurizot, I. Huc, *Angew. Chem. Int. Ed.* **2003**, *42*, 2738 – 2740; *Angew. Chem.* **2003**, *115*, 2844 – 2846; c) I. Okamoto, M. Nabeta, Y. Hayakawa, N. Morita, T. Takeya, H. Masu, I. Azumaya, O. Tamura, *J. Am. Chem. Soc.* **2007**, *129*, 1892 – 1893.
[10] a) Y. Hua, A. H. Flood, *J. Am. Chem. Soc.* **2010**, *132*, 12838 – 12840; b) Y. Wang, F. Bie, H. Jiang, *Org. Lett.* **2010**, *12*, 3630 – 3633; c) M. Barboiu, J.-M. Lehn, *Proc. Natl. Acad. Sci. USA* **2002**, *99*, 5201 – 5206; d) A.-M. Stadler, N. Kyritsaka, J.-M. Lehn, *Chem. Commun.* **2004**, 2024 – 2025.
[11] G. Lautrette, C. Aube, Y. Ferrand, M. Pipelier, V. Blot, C. Thobie, B. Kauffmann, D. Dubreuil, I. Huc, *Chem. Eur. J.* **2014**, *20*, 1547 – 1553.
[12] a) C. Zhan, J.-M. Léger, I. Huc, *Angew. Chem. Int. Ed.* **2006**, *45*, 4625 – 4628; *Angew. Chem.* **2006**, *118*, 4741 – 4744; b) H. Goto, Y. Furusho, E. Yashima, *J. Am. Chem. Soc.* **2007**, *129*, 9168 – 9174; c) R. Amemiya, N. Saito, M. Yamaguchi, *J. Org. Chem.* **2008**, *73*, 7137 – 7144; d) Y. Tanaka, H. Katagiri, Y. Furusho, E. Yashima, *Angew. Chem. Int. Ed.* **2005**, *44*, 3867 – 3870; *Angew. Chem.* **2005**, *117*, 3935 – 3938; e) H. Ito, Y. Furusho, T. Hasegawa, E. Yashima, *J. Am. Chem. Soc.* **2008**, *130*, 14008 – 14015.
[13] a) E. Berni, B. Kauffmann, C. Bao, J. Lefeuvre, D. M. Bassani, I. Huc, *Chem. Eur. J.* **2007**, *13*, 8463 – 8469; b) Q. Gan, C. Bao, B. Kauffmann, A. Grélard, J. Xiang, S. Liu, I. Huc, H. Jiang, *Angew. Chem. Int. Ed.* **2008**, *47*, 1715 – 1718; *Angew. Chem.* **2008**, *120*, 1739 – 1742; c) Y. Ferrand, A. M. Kendhale, J. Garric, B. Kauffmann, I. Huc, *Angew. Chem. Int. Ed.* **2010**, *49*, 1778 – 1781; *Angew. Chem.* **2010**, *122*, 1822 – 1825.
[14] E. Berni, J. Garric, C. Lamit, B. Kauffmann, J.-M. Léger, I. Huc, *Chem. Commun.* **2008**, 1968 – 1970.
[15] Y. Ferrand, N. Chandramouli, A. M. Kendhale, C. Aube, B. Kauffmann, A. Grélard, M. Laguerre, D. Dubreuil, I. Huc, *J. Am. Chem. Soc.* **2012**, *134*, 11282 – 11288.
[16] R. Krämer, J.-M. Lehn, A. Marquis-Rigault, *Proc. Natl. Acad. Sci. USA* **1993**, *90*, 5394 – 5398.
[17] M. L. Singleton, N. Castellucci, S. Massip, B. Kauffmann, Y. Ferrand, I. Huc, *J. Org. Chem.* **2014**, *79*, 2115 – 2122.
[18] The introduction of functional groups that do not interfere with double-helix formation on an analogue of **1** would enable the formation of a true heterodimer with **2**, whereas **2**⊂**1** might be considered a pseudo-homodimer in that it contains two different strands, but two identical $\mathbf{A}_5$ segments.